

Diurnal and seasonal variations of ultrafine particle formation in anthropogenic SO₂ plumes

Journal:	<i>Environmental Science & Technology</i>
Manuscript ID:	es-2009-03228a.R1
Manuscript Type:	Article
Date Submitted by the Author:	23-Dec-2009
Complete List of Authors:	Yu, Fangqun; State University of New York at Albany, ASRC



Diurnal and seasonal variations of ultrafine particle formation in anthropogenic SO₂ plumes

Fangqun Yu

Atmospheric Sciences Research Center, State University of New York, Albany, New York

Corresponding author phone: (518) 437-8767; e-mail: yfq@asrc.cestm.albany.edu

Abstract. The cloud condensation nuclei concentrations predicted by global aerosol models are sensitive to how the new particle formation in sub-grid anthropogenic SO₂ plumes is parameterized. Using a state-of-the-art kinetic nucleation model, we carried out two case studies to investigate the large difference in the number concentrations of ultrafine particles observed in the plumes from the Horne smelter: one in the summer and the other in the winter. Our model predicted particle number concentrations are in good agreement with observations for both cases, showing that the particle formation in the Horne smelter plumes is dominated by binary homogeneous nucleation (BHN) in the winter case and by ion-mediated nucleation (IMN) in the summer case. Further sensitivity studies reveal significant diurnal and seasonal variations of sulfate particle formation in the anthropogenic SO₂ plume, mainly associated with the corresponding variations of two key parameters – hydroxyl radical concentration ([OH]) and temperature. Nucleation in the plume is negligible at night because of very low [OH]. The BHN is significant when [OH] is relatively high or temperature is relatively low, and it is generally limited to the fresh plumes (within ~ 15 km from source), but it can generate very high number concentrations of ultrafine particles (peak values as high as 10⁵ - 10⁶ cm⁻³) under favorable conditions. The IMN generally dominates nucleation in the plume when [OH] is relatively low or temperature is relatively high, and it extends from fresh plume to more aged plume and produces 2-3×10⁴ cm⁻³ of nucleated particles. The implications of the results are discussed.

Introduction

The aerosol indirect radiative forcing, the most important source of uncertainties in assessing climate change (*I*), is largely determined by the number abundance of particles that can act as cloud condensation nuclei (CCN). At a given water supersaturation ratio, CCN number concentrations depend on the number size distribution and composition of atmospheric particles. Aerosol particles appear in the troposphere due to either in-situ nucleation (i.e., secondary particles) or direct emissions (i.e., primary particles). Most of the recent global aerosol simulations assume that 0-5% of anthropogenic sulfur species is emitted as sulfuric acid or sulfate and the rest is emitted as SO₂ (2-7). While this fraction of sulfate mass (f_{SO_4}) is called “primary sulfate”, it is actually secondary in nature because it is used to account for the sub-grid SO₂ oxidation and new particle formation. The above-mentioned global aerosol simulations show that the simulated tropospheric CCN abundance is sensitive to the parameterization of the new particle formation in sub-grid SO₂ plumes (especially in the source regions), and thus it is important to reduce the uncertainties in this parameterization.

Sulfur emission from power plants and smelters is a dominant anthropogenic sulfur source. Thorough airborne sampling of the SO₂ to sulfate conversion rate (r_{sc}) and sulfate particle formation in plumes from coal-fired power plants and smelters was undertaken in the late 1970s and early 1980s. Measurements reported by Wilson and McMurry (8) indicate that the formation of sulfate particles in the power plant plume depends strongly upon the time of day with none observed in plume parcels which were not exposed to sunlight. Wilson (9) reviewed measurements collected in twelve power plant and smelter plumes in Australia, Canada and the U.S., during warm and cold seasons, and during days and nights. In spite of the wide geographical, seasonal, background and source variations, Wilson (9) showed a distinct

1
2
3 difference in the observed day and night r_{sc} . The variability is significantly less for plumes with
4 similar exposure to sunlight dose (9), which is consistent with the fact that the dominant route of
5 oxidation of SO_2 in the gas phase is the reaction with the hydroxyl radical (OH) (10, 11).
6 Depending on the OH concentration ([OH]), r_{sc} can vary from $\ll 1\%/hr$ to $\sim 10\%/hr$ (11). It is
7 clear that the fractions of sulfur converted to sulfate during the sub-grid plume dilution ($f_{SO_4} =$
8 $r_{sc} \times \Delta t$) depend on [OH] and have clear diurnal variations. Sulfate particle formation in power
9 plant and smelter plumes has been characterized in a number of more recent field measurements
10 (12-15). Banic et al. (15) showed that the number concentration of ultrafine particles formed in
11 the same smelter plume differs significantly in winter and summer.

12
13 In addition to f_{SO_4} , the concentrations and sizes of nucleated particles in sub-grid
14 anthropogenic sulfur plumes are also expected to vary significantly. The mass of primary sulfate,
15 calculated from f_{SO_4} and the sulfur emission rate at a given grid box, is generally distributed into
16 two lognormal modes with the geometric mean diameters (d_g) and standard deviations (σ_g) of 10
17 nm and 1.6 for nucleation mode and 70 nm and 2.0 for condensation mode (16). As it has been
18 pointed out in Yu and Luo (7), most of the global aerosol studies assume that 15% of primary
19 sulfate mass is emitted into the nucleation mode (i.e., $f_{nucl} = 15\%$), while the rest is partitioned
20 into the condensation or accumulation mode. However, the reference cited in these studies (16-
21 17) showed that f_{nucl} is 5% (instead of widely used 15%) while the remaining of sulfate (formed
22 in sub-grid SO_2 plumes) condenses directly onto existing particles. Whitby et al. (16) derived the
23 typical values of d_g and σ_g , as well as f_{nucl} from limited measurements obtained in the Labadie
24 power plant plume near St. Louis, Missouri in 1976. It is clear that one can expect large
25 uncertainties in these parameters. Actually, Whitby et al. (16) showed that f_{nucl} derived from
26 measurements obtained in eight different plume crossings range from 1% to 9%. It should be
27
28
29
30
31
32
33
34
35
36
37
38
39
40
41
42
43
44
45
46
47
48
49
50
51
52
53
54
55
56
57
58
59
60

1
2
3 noted that the primary sulfate mass from the power plant is distributed into a log-normal mode
4 with $d_g=500$ nm and $\sigma_g=2.0$ in AeroCom inventory (18) but the physics or reason behind such an
5
6
7
8 assumption is unclear.
9

10 As far as we know, all the existing global aerosol studies assume a fixed f_{SO_4} , f_{nucl} , d_g and σ_g
11 for the whole simulation period over the whole globe (i.e., no diurnal, seasonal, and spatial
12 variations). Such an overly simplified representation of the sub-grid new particle formation is
13 likely to significantly over-predict the new particle formation in the local night time and lead to
14 large uncertainties in the spatiotemporal variations of predicted ultrafine particle number
15 concentration and CCN abundance. The main objective of this study is to improve our
16 understanding of the diurnal and seasonal variations of ultrafine sulfate particle formation in
17 power plant/smelter plumes through case and sensitivity studies. Such an understanding is
18 critical to improve the representation of sub-grid plume scale nucleation process and thus reduce
19 the uncertainties in the regional and global simulations of aerosol number abundance that is
20 important for the assessment of aerosol climatic and health impacts.
21
22
23
24
25
26
27
28
29
30
31
32
33
34
35
36

37 **Methodology**

38 We employ the most recent version of kinetic ion-mediated nucleation (IMN) model (19)
39 which is suitable for simulating the particle formation and evolution in diluting plumes, where
40 key parameters are changing. The IMN model contains binary homogeneous nucleation (BHN)
41 and it reduces to BHN when ion concentration is set to zero or when nucleation rate is much
42 larger than the ionization rate. The IMN model explicitly solves particle condensation growth
43 and coagulation (including the scavenging of freshly nucleated nanometer size particles by pre-
44 existing particles) (19). In the past, the kinetic IMN model has been successfully applied to study
45 particle formation and evolution in the plumes of aircraft exhaust and vehicular exhaust (20, 21).
46
47
48
49
50
51
52
53
54
55
56
57
58
59
60

1
2
3 There are five key parameters controlling new particle formation rate via IMN (22): sulfuric acid
4 vapor concentration ($[\text{H}_2\text{SO}_4]$), temperature (T), relative humidity (RH), ionization rate (Q), and
5
6 surface area of background particles (SB). $[\text{H}_2\text{SO}_4]$ in the power plant plumes depend on SO_2
7
8 concentration ($[\text{SO}_2]$), $[\text{OH}]$, SB, and plume dilution.
9
10

11
12 To simplify the problem, we treat the plume exhaust as a perturbed parcel of air subject to
13 dilution through mixing with ambient environment. The IMN model is a kinetic particle
14 formation and evolution model, and we run it as a box model along the trajectory of expanding
15 plume in an approach similar to previous simulations of particle evolution in aircraft plumes
16 (20). The dilution of the exhaust is represented as an increase in the cross-sectional area of the
17 plume by various mixing processes, and all of the constituents in the plume are assumed to be
18 uniformly mixed instantaneously across the entire cross section. While this approximation is
19 obviously crude, it may be rationalized as representing the bulk mean properties of the plume
20 (20). The plume dilution rate depends on the wind speed and boundary layer stability. There
21 exist a number of approaches to calculate plume dispersion process (23). One key consideration
22 is to specify the horizontal and vertical standard deviations (m) of the Gaussian distribution σ_y
23 and σ_z . In this study, we calculate σ_y and σ_z based on MESOPUFF II stability-dependent
24 dispersion curves (23):
25
26
27
28
29
30
31
32
33
34
35
36
37
38
39
40
41
42

$$\sigma_y = a_y x^{b_y}$$

$$\sigma_z = a_z x^{b_z}$$

43
44
45
46
47
48 where a_y , b_y , a_z , and b_z are the coefficients that depend on the Pasquill-Gifford-Turner (PGT)
49 stability class (Table 2-8 in ref. 23). x is the downwind distance.
50
51

52
53 The initial $[\text{SO}_2]$ can be calculated based on SO_2 emission rate (kg SO_2/hr), initial plume
54 cross section area, and wind speed. Apparently $[\text{SO}_2]$ in different plumes is expected to vary
55
56
57
58
59
60

1
2
3 significantly due to difference in SO₂ source rate and initial plume cross section and dispersion
4
5 rate. The conversion of SO₂ into sulfuric acid is calculated based on the reactions of SO₂ with
6
7 OH. It should be noted that [OH] in the concentrated plume stages (plume age ~ 10 s) is
8
9 generally 2-3 orders of magnitudes lower than those in the background air because the depletion
10
11 of ozone near the source region (24-26). [OH] in the plume approaches to [OH]_{amb} around plume
12
13 age of 300 – 600 s. To take into account of this, we use the plume age dependent [OH] profile
14
15 given in Cocks and Fletcher (24) to scale the [OH] in the fresh plume. Since SO₂ together with
16
17 [OH] determine the H₂SO₄ production rate, the impact of [SO₂] variations on nucleation at fixed
18
19 OH can be seen from the impact of [OH] variations at fixed [SO₂].
20
21
22
23
24

25 26 **Results and Discussion**

27
28 It is apparent from previous section that many parameters controlling new particle formation
29
30 in power plant or smelter plumes can have large spatial and temporal variations. The focus of the
31
32 present study is on the impact of two key parameters controlling the diurnal and seasonal
33
34 variations of sulfate particle formation in the power plant plume: [OH] and T.
35
36

37
38 **Simulations and Comparisons with Measurements: Case Studies.** We first carry out case
39
40 studies of two flight measurements taken in the plumes from the Horne smelter (one in summer –
41
42 7/28/2000 and the other in winter – 2/19/2000, ref. 15), aiming to understand the observed large
43
44 difference in the number concentrations of ultrafine particles formed in two different seasons.
45
46 The sulfur emission rate for the Horne smelter is taken from Savard et al. (27). The metrological
47
48 parameters (T, RH, and wind speed V), and ambient [OH] and surface area of background
49
50 particles (SB) needed for the plume simulations are based on GEOS-Chem simulations (7).
51
52 GEOS-Chem uses assimilated meteorological data from the NASA Goddard Earth Observing
53
54 System and contains many state-of-the-art modules treating various chemical and particle
55
56
57
58
59
60

1
2
3 processes (28-30). The values of T, RH, V, [OH], and SB in the Horne smelter region during the
4
5 periods when measurements were taken (15) are 293 K, 65%, 5 m/s, $2 \times 10^6 \text{ cm}^{-3}$, and 140
6
7 $\mu\text{m}^2\text{cm}^{-3}$ respectively on 7/28/2000 (summer case) and 267 K, 78%, 7.5 m/s, 10^6 cm^{-3} , and 150
8
9 $\mu\text{m}^2\text{cm}^{-3}$ respectively on 2/19/2000 (winter case). The values of T, RH, and V for the two periods
10
11 are overall consistent with the meteorology data in the region archived at weather underground
12
13 (<http://www.wunderground.com>). Based on assumed size distributions of pre-existing particles
14
15 (see Section 2), SB values of 140–150 $\mu\text{m}^2\text{cm}^{-3}$ give total particle number concentration of ~
16
17 2400 cm^{-3} , consistent with several thousand per cm^3 of background particles observed in the
18
19 upper wind (15). The ionization rate is assumed to be 10 ion-pairs $\text{cm}^{-3}\text{s}^{-1}$ (31). The background
20
21 aerosol is assumed to have a bimodal log-normal distribution with mean dry diameter and
22
23 standard deviation of $d_1=60 \text{ nm}$, $\sigma_1=1.6$ and $d_2=200 \text{ nm}$, $\sigma_2=1.8$. The ratio of total number
24
25 concentration of mode 1 (N_1) to that of mode 2 (N_2) is assumed to be 100:3 and the exact values
26
27 of N_1 and N_2 are determined based on assumed SB values. Initial primary particles from
28
29 combustion (at plume age = 0) are assumed to have a bimodal log-normal distribution with
30
31 $N_1=10^6 \text{ cm}^{-3}$, $d_1=100 \text{ nm}$, $\sigma_1=1.6$ and $N_2=10^4 \text{ cm}^{-3}$, $d_2=1000 \text{ nm}$, $\sigma_2=1.8$ (32), which gives a total
32
33 surface area of $\sim 10^5 \mu\text{m}^2 \text{ cm}^{-3}$. The influence of uncertainties in the assumed ionization rates,
34
35 size distributions of background particles and initial plume particles on simulated results is
36
37 assessed in Supporting Information.
38
39
40
41
42
43
44

45
46 Figures 1 and 2 show $[\text{SO}_2]$, $[\text{H}_2\text{SO}_4]$, number concentrations of condensation nuclei with
47
48 diameter larger than 3 nm (CN3) and 15 nm (CN15), and particle number size distributions as a
49
50 function of plume distances from source (x), simulated with the kinetic IMN model for the two
51
52 study cases. For comparisons, the observed SO_2 concentrations for the winter case and the
53
54 observed CN15 for both winter and summer case (estimated from Figs. 3 & 4 in ref. 15) are also
55
56
57
58
59
60

1
2
3 marked in Figs. 1a and 1b. No measured values of $[\text{SO}_2]$ for the summer case were reported in
4
5 Banic et al. (15). It is clear that the simulated $[\text{SO}_2]$ for the winter case is consistent with
6
7 measurements at $x=10$ km and 20 km, suggesting that plume dilution parameterization is
8
9 reasonable. $[\text{SO}_2]$ in the summer case is a factor of ~ 1.5 higher than that in the winter case
10
11 because of lower wind speed. The particle number concentration in the plume near the source is
12
13 higher due to emission of primary particles but drops to ambient level within a distance of ~ 3
14
15 km from source because of dilution. As a result of higher $[\text{SO}_2]$ and $[\text{OH}]$ and thus H_2SO_4
16
17 production rate, $[\text{H}_2\text{SO}_4]$ is a factor of ~ 3 higher in the summer case. However, nucleation is
18
19 much stronger in the winter case due to the lower temperature. In the winter case, the peak value
20
21 of CN3 reaches $1.7 \times 10^5 \text{ cm}^{-3}$ at $x \sim 8$ km and then decreases gradually as a result of dilution
22
23 and coagulation. In the summer case, CN3 reaches $\sim 2 \times 10^4 \text{ cm}^{-3}$ at $x \sim 5$ km and thereafter
24
25 slightly increases with plume age despite dilution, indicating continuous particle nucleation and
26
27 growth in the plume (also see Fig. 2b). It is clear from Fig. 1 that the predicted CN15 agrees
28
29 quite well with observations for both seasons and our model captures the large difference in the
30
31 observed CN15 between the two seasons. Our model simulations confirm the significant new
32
33 particle formation in the smelter plume and total particle number concentrations in the plume can
34
35 exceed that of background by a factor of ~ 10 or more.
36
37
38
39
40
41
42

43
44 The relative contribution of BHN and IMN to the particles formed in the SO_2 plumes can be
45
46 determined by setting the ionization rate to zero (see Fig. S1 in Supporting Information). For the
47
48 two case studies shown in Figs. 1 and 2, our analysis indicates that the particle formation is
49
50 dominated by BHN in the winter case while it is dominated by IMN in the summer case. In the
51
52 winter case, the peak nucleation rate can reach up to $\sim 700 \text{ cm}^{-3} \text{ s}^{-1}$ at $x \sim 6$ km because of lower
53
54 T and these nucleated particles grow to ~ 10 nm at $x=10$ km (Fig. 2a). In the summer case, the
55
56
57
58
59
60

1
2
3 particle growth rate is larger because of higher $[H_2SO_4]$ and the new particles formed near source
4
5 ($x < \sim 10$ km) can grow to ~ 40 nm (Fig. 2b). At $x > 10$ km, nucleation continues (mainly via IMN)
6
7
8 in both cases. Most of the new particles formed at $x > 10$ km in the winter case are scavenged by
9
10 the large concentration of particles nucleated at $x < 10$ km. In contrast, in the summer case, most
11
12 of the particles formed at $x > 10$ km grow to a size of ~ 10 nm and these particles dominate the
13
14 total particle number concentration at $x = 30$ km (Fig. 2b). Figure 2 shows that the nucleation
15
16 mode particles at $x = 30$ km in both cases have median sizes of ~ 15 nm, slightly larger than the
17
18 widely used parameterization ($d_g = 10$ nm) given by Whitby et al. (16). It is also clear from Fig.
19
20 2 that the nucleation mode particle size distributions change as the plume evolves, and the total
21
22 number concentration and standard deviation of nucleation mode particles differ significantly for
23
24 the winter and summer cases.
25
26
27
28

29
30 It should be noted that the case study simulations shown in Figs. 1 and 2 are subject to some
31
32 uncertainties associated with the assumed values of some input parameters such as ionization
33
34 rates, size distributions of background particles and initial plume particles (Supporting
35
36 Information). Nevertheless, these uncertainties do not affect our conclusion about the dominance
37
38 of IMN in the summer case and BHN in the winter case. While SO_2 oxidation rate and hence
39
40 H_2SO_4 concentration are lower in the winter case, BHN leads to very high nucleation rate as a
41
42 result of low temperature which explains why the particle number concentrations observed in the
43
44 plumes from the Horne smelter in the winter season are much larger than those in the summer
45
46 case.
47
48
49

50
51 **Diurnal and Seasonal Variations: Sensitivity Studies.** In the two case study simulations
52
53 shown in Figs. 1 and 2, the $[OH]$ values are close to the peak values during the day. As we
54
55 pointed out in the Introduction, observations indicate that sulfate particle formation in
56
57
58
59
60

1
2
3 anthropogenic SO₂ plumes clearly have diurnal variations. [OH], the key factor controlling the
4 observed diurnal variations, also have large spatial variations and peak [OH] concentration can
5 exceed 1×10⁷ cm⁻³ at low latitudes. We have carried out sensitivity studies to investigate the
6 impact of [OH] values on formation and properties of sulfate particles in anthropogenic SO₂
7 plume. Figure 3 shows the predicted CN₃ as a function of distance from source (Figs. 3a, 3c) and
8 particle size distributions at x=30 km (Figs. 3b, 3d) under nine [OH] values range from 10⁴ – 10⁷
9 cm⁻³ and two temperatures (267 K and 293 K). To isolate the effect of T, all other parameters
10 (RH, wind speed, SB, etc.) are assumed to be the same for the simulations shown in Figs. 3a-b
11 and Figs. 3c-d.

12
13
14
15
16
17
18
19
20
21
22
23
24
25 As expected, [OH] has strong impact on new particle formation in SO₂ plume, not only on
26 the total number concentrations but also on the sizes of nucleated particles. The impact of T can
27 also clearly seen by comparing Figs.3a-b with Figs. 3c-d. Under the assumed conditions,
28 nucleation in the plume is negligible when [OH] < ~ 10⁴ cm⁻³ at T=267 K and when [OH] <
29 ~3×10⁴ cm⁻³ at T=293 K. A substantial amount of new particles are formed when [OH]>~ 10⁵
30 cm⁻³. IMN generally dominates and produces up to ~2-3×10⁴ cm⁻³ of particles when
31 [OH]<~5×10⁵ cm⁻³ at T=267 K and when [OH]<~5×10⁶ cm⁻³ at T=293 K. BHN becomes
32 significant at high [OH] and levels of [OH] for BHN to be important depend on T. At T=267 K
33 (representing winter condition), BHN can generate large amounts of ultrafine particles when
34 [OH]>~5×10⁵ cm⁻³, with peak concentrations reaching 10⁵-10⁶ cm⁻³ in the plume within a
35 distance of ~ 15 km from source. At T=293 K (representing summer condition), BHN becomes
36 important when [OH]>~5×10⁶ cm⁻³, but the degree of nucleation strength is much less than at
37 lower T. BHN is generally limited to the relatively fresh plumes (within ~ 15 km from source)
38 while IMN continues in the aged plumes, resulting in a bimodal size distribution of nucleated
39
40
41
42
43
44
45
46
47
48
49
50
51
52
53
54
55
56
57
58
59
60

1
2
3 particles (Figs. 3b and 3d). The nucleated particles of larger modes in Figs. 3b ($d_g > \sim 10$ nm) and
4
5 3d ($d_g > \sim 30$ nm) are mainly from BHN (nucleated earlier and have more time to grow) while
6
7 those of smaller mode are resulted from IMN.
8
9

10 Our case and sensitivity studies show clear diurnal and seasonal variations of new particle
11 formation in anthropogenic SO₂ plumes, mainly as a result of variations in [OH] and T. While
12 other parameters (such as RH, SO₂ emission rate, wind speed, mixing process, and surface area
13 of pre-existing particles) will also affect particle formation in the SO₂ plumes, their contributions
14 to the diurnal and seasonal variations are expected to be relatively small. In a given SO₂ plume,
15 night time nucleation in the SO₂ plume is negligible because of very low [OH], and day time
16 nucleation strength depends on [OH] and T. The IMN generally dominates nucleation in the
17 plume when [OH] is relatively low and T is relatively high, and it can last for several hours and
18 generate $2-3 \times 10^4$ cm⁻³ of nucleated particles. The BHN can become significant when [OH] is
19 relatively high and T is relatively low, and it is generally limited to the relatively fresh plumes
20 (within ~ 15 km from source) but it can generate very high concentrations of ultrafine particles
21 (peak values as high as 10^5-10^6 cm⁻³) under certain conditions. The relative and absolute
22 contributions of BHN and IMN to new particles formed in the SO₂ plume mainly depend on T
23 and [H₂SO₄], with the latter controlled by [OH], [SO₂], and surface area of pre-existing particles
24 in the plume. It should be noted that BHN may become dominant in the summer and IMN in the
25 winter under certain conditions.
26
27
28
29
30
31
32
33
34
35
36
37
38
39
40
41
42
43
44
45
46
47

48 **Implications.** The key processes and parameters controlling the formation and properties of
49 nucleated particles in the anthropogenic SO₂ plumes are poorly understood. The diurnal and
50 seasonal variations of ultrafine sulfate particle formation in power plant/smelter plumes are
51 investigated in the present study, with a state-of-the-art kinetic nucleation model. Our results
52
53
54
55
56
57
58
59
60

1
2
3 show that the BHN, while is generally unimportant to particle formation in the ambient
4 atmosphere, can lead to very large concentrations ($> 10^5 \text{ cm}^{-3}$) of ultrafine particles in relatively
5 fresh anthropogenic SO_2 plumes under suitable conditions (low T, high [OH]). It should be noted
6 that the BHN component of the IMN model, on which the current research is based, is
7 constrained by multiple independent laboratory data sets and has much smaller uncertainty
8 compared to previous BHN models (33). Ammonia and certain organic species are known to be
9 able to enhance the BHN and it remains to be investigated how much these species can enhance
10 nucleation in anthropogenic SO_2 plumes. More comparisons of theoretical predictions with
11 detailed measurements are needed to further advance our understanding of nucleation process in
12 anthropogenic SO_2 plumes.
13
14
15
16
17
18
19
20
21
22
23
24
25

26
27 Our case and sensitivity studies indicate that the concentrations and sizes of ultrafine sulfate
28 particles formed in the anthropogenic SO_2 plumes have large temporal (diurnal and seasonal) and
29 spatial variations. Previous global aerosol studies assuming fixed (i.e., no spatiotemporal
30 variations) parameterizations of sub-grid new particle formation in the anthropogenic SO_2 plume
31 are subject to large uncertainties in the predicted ultrafine particle number concentration and
32 CCN abundance near source regions. Further research is needed to develop suitable
33 parameterization of sub-grid plume scale new particle formation which considers its
34 spatiotemporal variations. Application of such parameterization is necessary to improve the
35 ability of the regional and global size-resolved aerosol models in predicting the spatiotemporal
36 variations of aerosol number concentration and CCN abundance, which is important for
37 assessing aerosol climatic and health impacts.
38
39
40
41
42
43
44
45
46
47
48
49
50
51

52
53
54
55
56 **Acknowledgments.** This study is supported by grants from NASA and NSF.
57
58
59
60

Supporting Information Available

Table S1 contains the values assumed in the baseline and sensitivity study cases for the following parameters: surface area of background aerosol, the ratio of the total number concentration of mode 1 to that of mode 2 of background aerosol, surface area of initial particles in the plume, and ionization rate. Figure S1 shows the influence of uncertainties in the above mentioned parameters on the simulated evolution of particle number concentrations in the SO₂ plume from the Horne smelter: one in summer and the other in winter. This material is available free of charge via the Internet at <http://pubs.acs.org>.

Literature Cited

- (1) IPCC, Climate Change 2007. *The Physical Scientific Basis*; S. Solomon, D. Qin, et al. Eds. Cambridge Univ. Press, New York, 2007.
- (2) Adams, P. J.; Seinfeld, J. H. Disproportionate impact of particulate emissions on global cloud condensation nuclei concentrations. *Geophys. Res. Lett.* **2003**, *30*, 1239, doi:10.1029/2002GL016303.
- (3) Spracklen, D. V.; Pringle, K. J.; Carslaw, K. S.; Chipperfield, M. P.; Mann, G. W. A global off-line model of size-resolved aerosol microphysics: II. Identification of key uncertainties. *Atmos. Chem. Phys.* **2005**, *5*, 3233–3250.
- (4) Pierce, J. R.; Adams, P. J. Global evaluation of ccn formation by direct emission of sea salt and growth of ultrafine sea salt. *J. Geophys. Res.* **2006**, *111*, D06203, doi:10.1029/2005JD006186.

- 1
2
3
4
5
6
7
8
9
10
11
12
13
14
15
16
17
18
19
20
21
22
23
24
25
26
27
28
29
30
31
32
33
34
35
36
37
38
39
40
41
42
43
44
45
46
47
48
49
50
51
52
53
54
55
56
57
58
59
60
- (5) Makkonen, R.; Asmi, A.; Korhonen, H.; Kokkola, H.; Järvenoja, S.; Räisänen, P.; Lehtinen, K.E.J.; Laaksonen, A.; Kerminen, V.-M.; Järvinen, H.; et al. Sensitivity of aerosol concentrations and cloud properties to nucleation and secondary organic distribution in ECHAM5-HAM global circulation model. *Atmos. Chem. Phys.* **2009**, *9*, 1747-1766.
- (6) Wang, M.; Penner, J. E. Aerosol indirect forcing in a global model with particle nucleation. *Atmos. Chem. Phys.* **2009**, *9*, 239-260.
- (7) Yu, F.; Luo, G. Simulation of particle size distribution with a global aerosol model: Contribution of nucleation to aerosol and CCN number concentrations. *Atmos. Chem. Phys.* **2009**, *9*, 7691-7710.
- (8) Wilson, J. C.; McMurry, P.H. Studies of aerosol formation in power plant plumes. II. Secondary aerosol formation in the Navajo Generating Station plume. *Atmos. Environ.* **1981**, *15*, 2329-2339.
- (9) Wilson, W. E. Sulfate formation in point source plumes: A review of recent studies. *Atmos. Environ.* **1981**, *15*, 2573-2581.
- (10) Hegg, D.A.; Hobbs, P.V. Measurements of gas-to-particle conversion in the plumes from five coal-fired electric power plants. *Atmos. Environ.* **1980**, *14*, 99-116.
- (11) Hewitt, C. N. The atmospheric chemistry of sulphur and nitrogen in power station plumes. *Atmos. Environ.* **2001**, *35*, 1155-1170.
- (12) Brock, C. A.; Trainer, M.; Byerson, T. B.; Neuman, J. A.; Parrish, D. D.; Holloway, J.S., Nicks Jr., D.K.; Frost, G.J.; Hübler, G.; Fehsenfeld, F.C.; et al. Particle growth in urban and industrial plumes in Texas. *J. Geophys. Res.* **2003**, *108*, 4111, doi:10.1029/2002JD002746.
- (13) Brock, C. A., Washenfelder, R. A.; Trainer, M.; Byerson, T. B.; Wilson, J. C.; Reeves, J.M.; Huey, L.G.; Holloway, J.S.; Parrish, D.D.; Hübler, G.; Fehsenfeld, F.C. Particle growth in

- 1
2
3 the plumes of coal-fired power plants. *J. Geophys. Res.* **2002**, *107*(D12), 4155,
4
5 doi:10.1029/2001JD001062.
6
7
8 (14) Springston, S. R.; Kleinman, L. I.; Brechtel, F.; Lee, Y.N.; Nunnermacker, L. J.; Wang, J.
9
10 Chemical evolution of an isolated power plant plume during the TexAQS 2000 study. *Atmos.*
11
12 *Environ.* **2005**, *39*, 3431-3443.
13
14
15 (15) Banic, C.; Leaitch, W. R.; Strawbridge, K.; Tanabe, R.; Wong, H.; Gariépy, C.; Simonetti,
16
17 A.; Nejedly, Z.; Campbell, J.L.; Lu, J.; et al. The physical and chemical evolution of aerosols
18
19 in smelter and power plant plumes: An airborne study. *Geochemistry: Exploration,*
20
21 *Environment, Analysis* **2006**, *6*, 111-120.
22
23
24 (16) Whitby, K. T.; Cantrell, B. K.; Kittelson, D. B. Nuclei formation rates in a coal-fired power
25
26 plant plume. *Atmos. Environ.* **1978**, *12*, 313-321.
27
28
29 (17) Whitby, K. The physical characteristics of sulfur aerosols. *Atmos. Environ.* **1978**, *12*, 135–
30
31 159.
32
33
34 (18) Dentener, F.; Kinne, S.; Bond, T.; Boucher, O.; Cofala, J.; Generoso, S.; Ginoux, P.;
35
36 Gong, S.; Hoelzemann, J. J.; Ito, A.; et al.: Emissions of primary aerosol and precursor gases
37
38 in the years 2000 and 1750 prescribed data-sets for AeroCom. *Atmos. Chem. Phys.* **2006**, *6*,
39
40 4321-4344.
41
42 (19) Yu, F. From molecular clusters to nanoparticles: Second-generation ion-mediated
43
44 nucleation model. *Atmos. Chem. Phys.* **2006**, *6*, 5193-5211.
45
46 (20) Yu, F.; Turco, R. P. The formation and evolution of aerosols in stratospheric aircraft plumes:
47
48 Numerical simulations and comparisons with observations, *J. Geophys. Res.*, **1998**, *103*, 25,915-
49
50 25,934.
51
52 (21) Yu, F. Chemiions and nanoparticle formation in diesel engine exhaust. *Geophys. Res. Lett.*
53
54 **2001**, *28*, 4191-4194.
55
56
57
58
59
60

- 1
2
3
4
5
6
7
8
9
10
11
12
13
14
15
16
17
18
19
20
21
22
23
24
25
26
27
28
29
30
31
32
33
34
35
36
37
38
39
40
41
42
43
44
45
46
47
48
49
50
51
52
53
54
55
56
57
58
59
60
- (22) Yu, F. Ion-mediated nucleation in the atmosphere: Key controlling parameters, implications, and look-up table. *J. Geophys. Res.* **2009**, doi:10.1029/2009JD012630, in press.
- (23) Scire., J.; Strimaitis, D. G.; Yamartino, R. J. *A User's Guide for the CALPUFF Dispersion Model (Version 5)*, 2000.
- (24) Cocks, A. T.; Fletcher, I. S. Major factors influencing gas=phase chemistry in power plant plumes during long range transport – II. Release time and dispersion rate for dispersion into an “urban” ambient atmosphere. *Atmos. Environ.* **1989**, *23*, 2801-2812.
- (25) Janssen, L.H.J.M.; Nieuwstadt, F.T.M.; Donze, M. Time scales of physical and chemical processes in chemically reactive plumes. *Atmos. Environ.* **1990**, *24A*, 2861-2874.
- (26) Kerminen, V.M.; Wexler, A. S. The occurrence of sulfuric acid-water nucleation in plumes: urban environment. *Tellus* **1996**, *48B*, 65-82.
- (27) Savard, M. M.; Bonham-Carter, G. F.; Banic, C. M. A geoscientific perspective on airborne smelter emissions of metals in the environment: an overview. *Geochemistry: Exploration, Environment, Analysis* **2006**, *6*, 99-109.
- (28) Bey, I.; Jacob, D. J.; Yantosca, R. M.; Logan, J. A.; Field, B.; Fiore, A. M.; Li, Q.; Liu, H.; Mickley, L. J.; Schultz M. Global modeling of tropospheric chemistry with assimilated meteorology: Model description and evaluation. *J. Geophys. Res.* **2001**, *106*, 23,073 – 23,096.
- (29) Park, R. J.; Jacob, D. J.; Field, B. D.; Yantosca, R. M.; Chin, M. Natural and transboundary pollution influences on sulfate-nitrate-ammonium aerosols in the United States: Implications for policy. *J. Geophys. Res.* **2004**, *109*, D15204, doi:10.1029/2003JD004473.
- (30) Evans, M. J.; Jacob, D. J. Impact of new laboratory studies of N₂O₅ hydrolysis on global model budgets of tropospheric nitrogen oxides, ozone, and OH. *Geophys. Res. Lett.* **2005**, *32*, L09813.

1
2
3 (31) Reiter, R. *Phenomena in Atmospheric and Environmental Electricity*. Elsevier, New York,
4
5 1992.
6

7
8 (32) Moisio, M.; Laitinen, A.; Hautanen, J.; Keskinen, J. Fine particle size distributions of seven
9
10 different combustion power plants. *J. Aerosol Sci.* **1998**, *29*, Suppl. 1, pp. S459-S460.
11

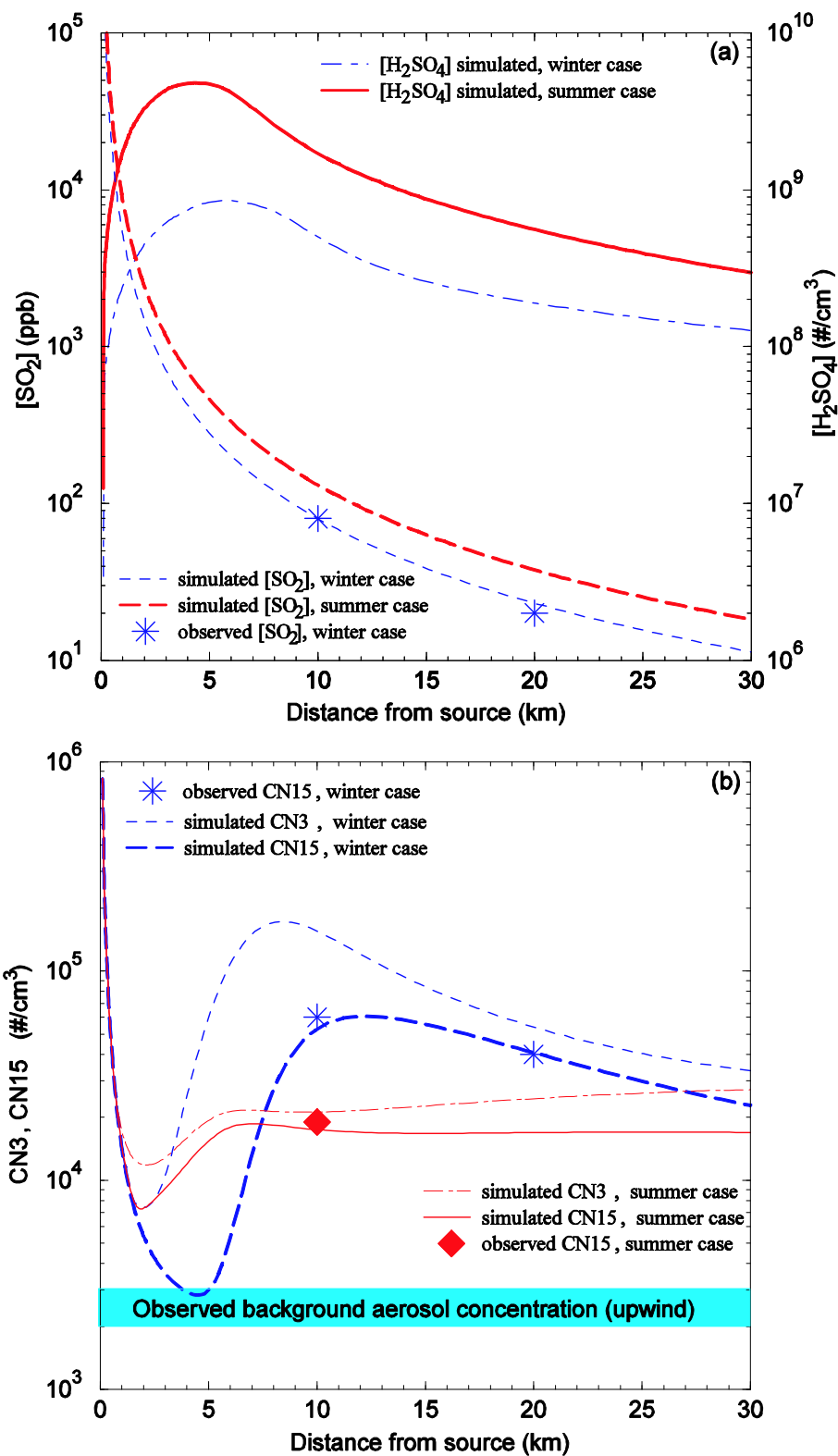
12
13 (33) Yu, F. An improved quasi-unary nucleation model for binary H₂SO₄-H₂O homogeneous
14
15 nucleation. *J. Chem. Phys.* **2007**, *127*, 054301.
16
17
18
19
20
21

22 **Figure Captions:**

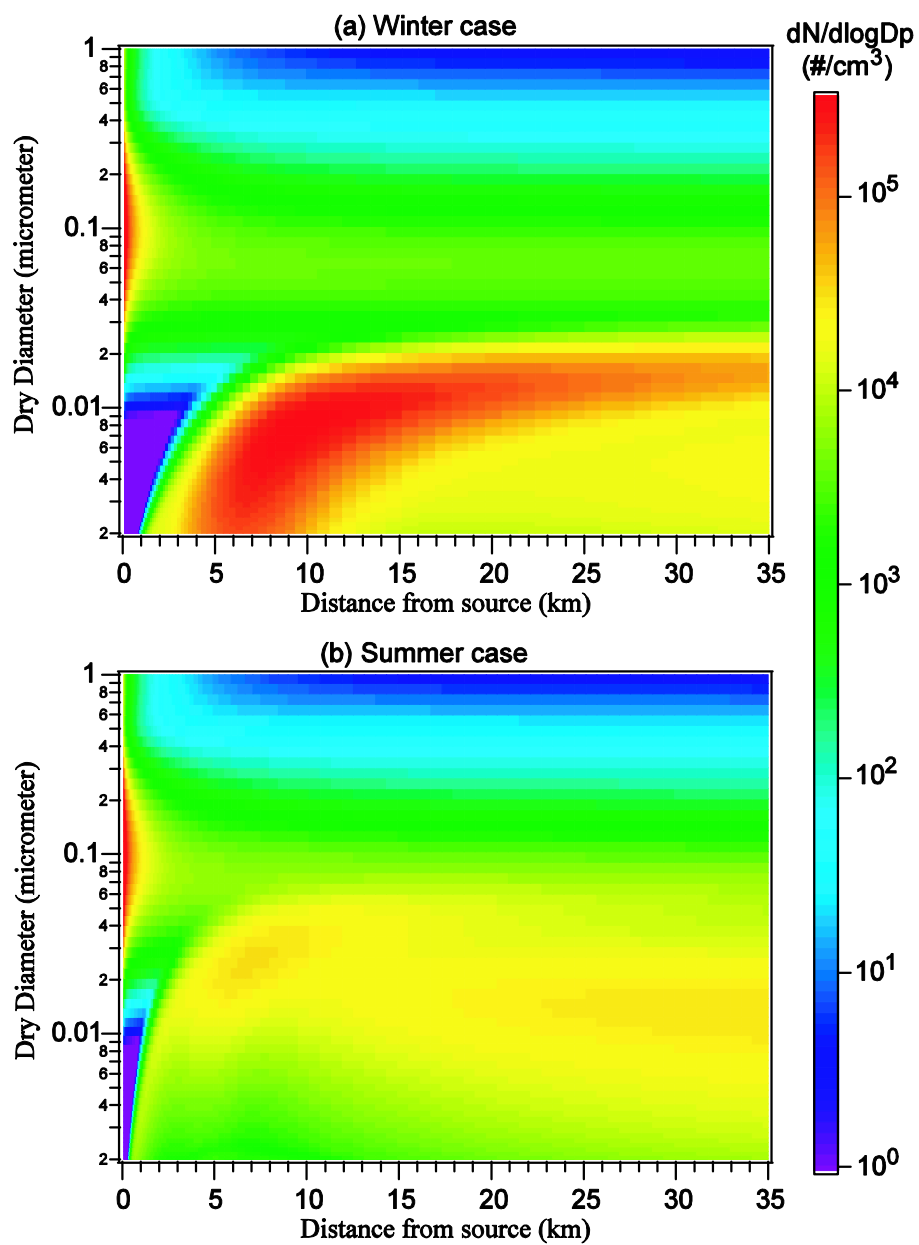
23
24 **Figure 1.** Simulated evolution (lines) of [SO₂], [H₂SO₄], and number concentrations of
25
26 condensation nuclei with diameter larger than 3 nm (CN3) and 15 nm (CN15) in the SO₂ plume
27
28 from the Horne smelter in two different seasons: one in summer (7/28/2000) and the other in
29
30 winter (2/19/2000). The symbols are the observed SO₂ concentrations for the winter case and the
31
32 observed CN15 for both winter and summer case (estimated from Figs. 3 & 4 in ref. 15).
33
34
35
36
37
38

39 **Figure 2.** Simulated evolution of particle number size distributions for the two cases shown in
40
41 Figure 1.
42
43
44
45

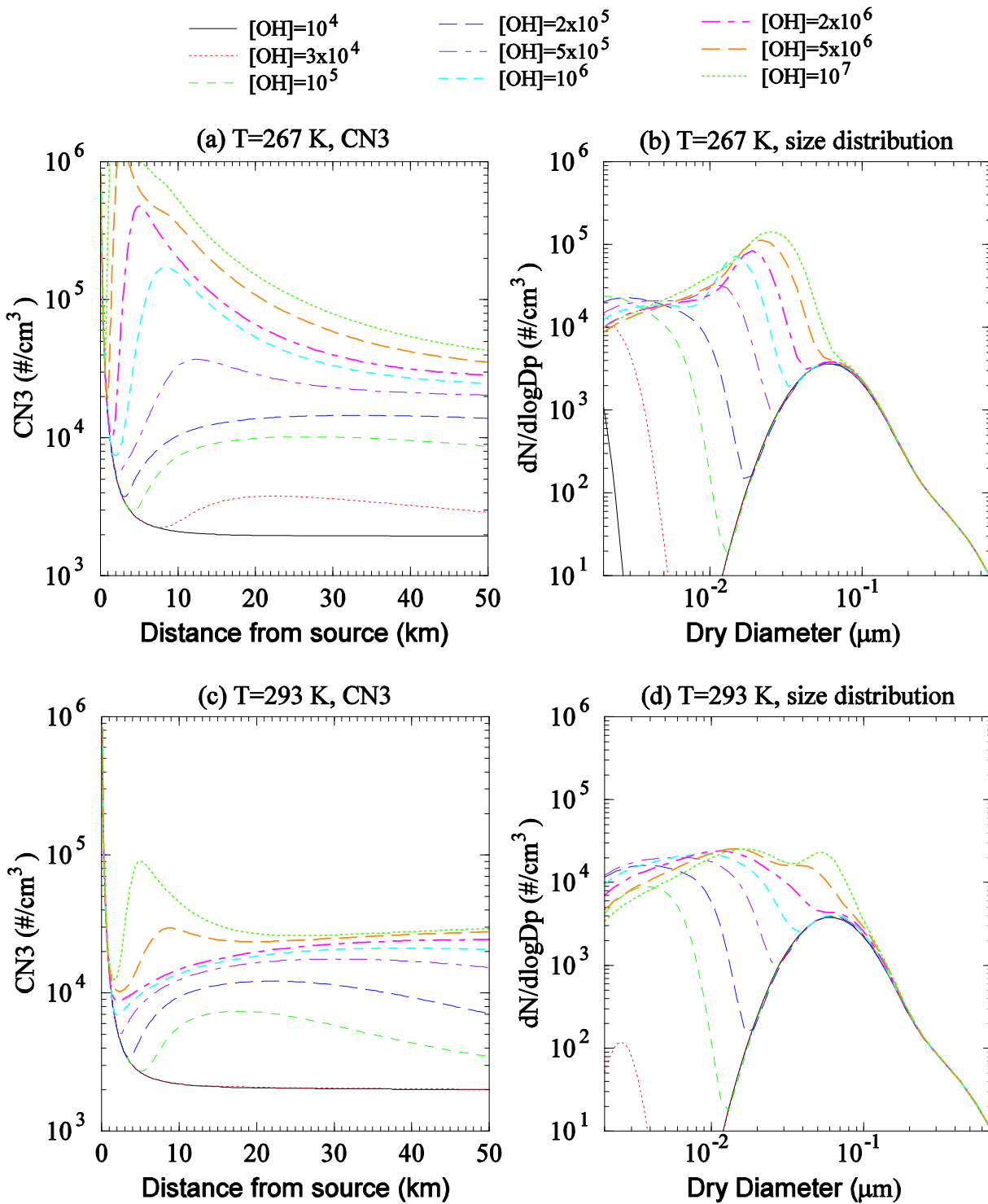
46 **Figure 3.** Predicted CN3 as a function of distance from source (a, c), and particle size
47
48 distributions at x=30 km (b, d) under nine [OH] value ranges and two temperatures (267 K and
49
50 293 K). All other parameters (wind speed, relative humidity, etc.) are assumed to be the same.
51
52
53
54
55
56
57
58
59
60



Yu, Figure 1



Yu, Figure 2



Yu, Figure 3

1
2
3 **Table of Contents brief:**
4
5
6
7

8 The diurnal and seasonal variations of ultrafine sulfate particle formation in power plant/smelter
9 plumes are investigated numerically through case and sensitivity studies.
10
11
12
13
14
15
16
17
18
19
20
21
22
23
24
25
26
27
28
29
30
31
32
33
34
35
36
37
38
39
40
41
42
43
44
45
46
47
48
49
50
51
52
53
54
55
56
57
58
59
60